Elastomeric Organosilicon Micronetworks

Frank Baumann, Bernhard Deubzer, Michael Geck, and Jochen Dauth

Wacker Chemie GmbH, D-84480 Burghausen, Germany

Manfred Schmidt*

Institute für Physikalische Chemie, Johannes Gutenberg-Universität Mainz, Jakob-Welder Weg 11, 55099 Mainz, FRG

Received March 26, 1997; Revised Manuscript Received August 18, 1997[⊗]

ABSTRACT: Trifunctional methyltrimethoxysilane and bifunctional dimethyldimethoxysilane monomers were cocondensed in water in the presence of surfactant. Strictly spherical micronetworks of narrow size distribution were obtained for particle sizes 10 nm < R < 30 nm. By special "endcapping" reactions all reactive SiOH groups were removed quantitatively, and the resulting micronetworks become soluble in common organic solvents like toluene, THF, or chloroform. For contents of trifunctional monomer larger than 50 mol % the particles do not swell irrespective of the choice of the solvent, whereas for lower mole fractions of trimethoxysilane an increasing swelling ratio is observed. Below 2.5 mol % trifunctional monomer the reaction within a microparticle remains subcritical and nonspherical, branched molecules are obtained. Subsequent addition of the bi- and trifunctional units leads to a micronetwork topology with different physical properties as compared to the simultaneously cocondensed one at identical overall particle composition. For instance, at 57 mol % trifunctional monomer content the "homogeneously" cross-linked microgel exhibits no glass transition before decomposition whereas the core−shell particle with linear chains in the core shows a weak glass transition at T_g = −107 °C.

Introduction

In recent publications[1,2] the preparation and properties of functionalized organosilicon microgels were described. In these studies trifunctional monomers such as X−Si$(OCH_3)_3$, with X = H, CH_3, CH═CH_2, CH_2-CH═CH_2, $(CH_2)_3SH$, $(CH_2)_3OOCCH{=}CH_2$, were homo- and cocondensed in the aqueous phase in the presence of surfactant. The resulting functionalized micronetworks were spherical and almost uniform in size in the regime of 5 nm < R < 20 nm and could be dissolved as single particles in common organic solvents like THF, toluene or CH_2Cl_2, if the residual SiO^- groups were quantitatively "endcapped" into "inert" Si−O−Si$(CH_3)_3$ moieties. Thus, highly functionalized microgels could be obtained bearing up to 30 000 functional groups per particle as well as core−shell structures with the functional groups located in the periphery of the microspheres. Due to the high cross-linking density the particles did not swell when dissolved in organic media. Also, similar to silcates the glass transition temperature is so high that it is never reached before decomposition of the organic moieties.

We here report on the preparation and characterization of "soft" micronetworks which do swell in organic solvents, exhibit glass transition temperatures as low as T_g = −115 °C, and behave like elastomers, accordingly.

Experimental Section

Synthesis. In the base-catalyzed system, 3 g (6.7 mmol) of the surfactant benzethonium chloride (Aldrich, M = 448 g/mol) was dissolved in 125 g of water (Milli-Q) and 0.75 mmol of NaOH (Fluka) was added. For methyltrimethoxysilane (T-units) contents less than 60 mol % of the amount of added NaOH is doubled to 1.5 mmol. Under vigerous stirring (KPG 300 rpm), 25 g of the respective monomer mixtures 0 ≤ D/T ≤ 1 (D = dimethyldimethoxysilane) were added slowly within 45 min at room temperature. The opalescent dispersion is continuously stirred for 5 h more. Removal of the surfactant at this stage generally leads to an insoluble precipitate because interparticle condensation takes place. In order to avoid interparticle condensation the Si−OH groups are first reacted with trimethylmethoxysilane (or a similar "endcapping" agent) before precipitation of the micronetworks as follows: 1.2 g of trimethylmethoxysilane (Wacker-Chemie GmbH, M = 104 g/mol) is added under stirring which is continued overnight. The dispersion is destabilized by addition of 50 mL of methanol and the precipitate is filtered off and washed several times with methanol in order to remove the surfactant. This procedure enables the micronetworks to dissolve in organic solvents like DMF, THF, dioxane, or toluene. It turns out that at this stage the reaction of the SiOH moities is not quantitative for micronetworks with more than 20 mol % T-units. Therefore the wet precipitate of such micronetworks is dissolved in 50 mL toluene, and 1.6 g of hexamethyldisilazane (Wacker-Chemie GmbH M = 161 g/mol) is added. The reaction mixture is stirred overnight, again. The resulting product is precipitated with 180 mL of methanol, filtered, predried, and finally dried in vacuo over night. Depending on the elastomer content, a white powder (T-unit > 50 mol %) or a colorless, sticky material is obtained.

The core−shell structures were prepared by subsequent addition of D- and T-units or vice versa. In order to avoid simultaneous cocondensation of the two monomers, the dispersion is stirred overnight before the second monomer is added and reacted to complete conversion. The samples with a core of linear chains and a cross-linked shell were prepared by adding 10 g (83.3 mmol) of dimethyldimethoxysilane (Wacker-Chemie GmbH, M = 120 g/mol) to the aqueous solution of surfactant and NaOH as described above. The solution is stirred at room temperature overnight before 15 g (110 mmol) of methyltrimethoxysilane (Wacker-Chemie GmbH, M = 136 g/mol) is added and stirred overnight, again. For the starlike structures (cross-linked core, shell of lenear chains) the respective quantities were 15 g of methyltrimethoxysilane followed by 10 g of dimethyldimethoxysilane. The endcapping reaction is then performed as described above.

Particle Characterization. Static and dynamic light-scattering measurements were performed with standard equipment utilizing an ALV SP-86 goniometer, an ALV 3000 correlator, and a Spectra Physics 20ll-s Krypton ion laser light source (647.1 nm wavelength, 500 mW power). Alternatively, for some dynamic light scattering measurements an ALV 5000 correlator and an ATLAS Nd-YAG laser (532,0 nm, 80 mW

[⊗] Abstract published in *Advance ACS Abstracts,* October 15, 1997.

S0024-9297(97)00415-4 CCC: $14.00

Table 1. Apparent Refractive Index Increments Measured in Water (See Appendix) and the Refractive Index Increments Measured in Toluene of the μ-Networks for Different Mole Fractions of D-Units, X_D

X_D	$dn/dc^{app}(H_2O)$	dn/dc(toluene)
0	0.1084	−0.0505
0.2		−0.0556
0.3	0.1111	
0.5		−0.0764
0.7	0.1147	−0.0797
0.8		−0.0921
0.95		−0.0998
1.0	0.1175	−0.1000

output power) were utilized. Correlation functions were analyzed by the method of cumulants.

All samples described here exhibit normalized second cumulants of $\mu_2 < 0.05$, and no angular dependence of the diffusion coefficients is observed. Before measurement the aqueous dispersions were diluted with 10^{-4} *m* KBr to concentrations 0.05 g/L < *c* < 0.3 g/L and were filtered through 0.22 μm Millex GS filters into the "dustfree" cylindrical Suprasil cuvettes with 10 mm outer diameter. The solutions in organic solvents, mostly toluene, were prepared in the same concentration range and were filtered through 0.2 μm Millex FGN Teflon filters. The refractive index increments were measured with a special, home-built interferometer utilizing a laser diode (Toshiba, wavelength $\lambda = 650$ nm)[3] and are listed in Table 1.

Thermal Analysis. The glass transition temperatures were determined with a Mettler TA 3000 instrument. In order to ensure a similar thermal history, all samples were heated up to 150 °C and than cooled down to −150 °C. The actual measurements were then performed from −150 to +150 °C. All cooling and heating rates were kept constant at 10 K per minute.

Results and Discussion

Light scattering results on the aqueous dispersion and on the "endcapped" microgels dissolved in toluene are summarized in Table 2. The aqueous dispersions exhibit a mean ratio $\rho_{LS} = R_g/R_h$ (with R_g the radius of gyration and R_h the hydrodynamic radius) of 0.80 which is slightly larger than the theoretical value $\rho_{LS} = 0.775$ for monodisperse hard spheres. The slightly larger values could well originate from the small, but finite polydispersities of the spheres. In toluene, the mean value of ρ_{LS} increases to 0.83, which is still close to the hard sphere value although for increasing D-content the particles start to swell. The swollen spheres rather resemble soft spheres which, however, within the time window of the correlator do not show pronounced internal modes of motion. Only for very small cross-linking densities below 2.5 mol % trifunctional monomer does the strong decrease in molar mass and significant increase of the ratio ρ_{LS} indicate that branching reaction within a microparticle remains subcritical.

One remarkable result is obtained for the condensation of pure dimethyldimethoxysilane which leads to a linear poly(dimethylsiloxane) of extremely high molar mass, i.e. $M_w = 70\,000$ g/mol. In a condensation reaction this high molar mass is achieved only if the conversion is in the order of 0.998! The molar mass distribution determined by GPC via polystyrene calibration was determined to $M_w/M_n = 1.8$ which is within the uncertainty close to the expected Schulz-Flory value.

Network Formation and Particle Size. Usually, polymerizations in μ-emulsion are characterized by the fleet ratio $S \equiv$ [surfactant]/[monomer]. Within a certain range of *S* values, stable dispersions are obtained, the size of which increases with decreasing *S*. A simple geometric calculation was found to quantitatively describe the size of the particles in dispersion as function of *S*.[4,5] Although the condensation reaction in the presence of surfactant does not represent a polycondensation in μ-emulsion, variation of the fleet ratio does allow the preparation of μ-networks with different size.[1] For the present system, an ambiguity concerning the precise definition of *S* results, because the monomer molar mass is significantly higher than the molar mass of the repeating unit in the resulting μ-network, as discussed in more detail below. Therefore in the present context the fleet ratio is given in terms of the weight concentration of the repeating unit under the approximate assumption of full conversion of all functional groups.

Also for the condensation reaction applied here the particle size increases with decreasing fleet ratio. The stability limits depend on the dispersion concentration, on the chemical composition of the monomers, and on other, more subtle effects like amount of catalyst, temperature and how quick the monomers are added. For pure trimethoxysilane (T-units) stable dispersions are obtained for $0.06 \le S \le 0.3$ at 10% solid content, whereas for pure dimethyldimethoxysilane (D-units) stable dispersions are formed for $S \ge 0.2$, only. In order to keep the solid content constant we have varied the ratio of trifunctional to bifunctional monomers from 0 to 100% at a constant fleet ratio $S = 0.25$. As shown in Figure 1 the size of the dispersion particles increases with increasing content of D-units until a maximum is found at about 99% D-units, which is confirmed by the

Table 2. Characterization of the Organosilicon μ-Networks in Aqueous Dispersion and of the Swollen μ-Networks in Toluene

T-units	10^{-4} *m* KBr					toluene				
(mol %)	R_h (nm)	R_g (nm)	ρ_{LS}	$M_w^D \times 10^6$ (g/mol)	ρ_d^D (g/cm^3)	R_h (nm)	R_g (nm)	ρ_{LS}	$M_w \times 10^6$ (g/mol)	ρ_d (g/cm^3)
100	10.6	<10[a]	<0.9	1.14	0.45	10.0	<10[a]	<1	2.0	0.82
70	11.2	<10[a]	<0.9	0.88	0.30	10.4	<10[a]	<0.96	2.10	0.74
50	12.7	11.0	0.86	1.23	0.26	11.7	<10[a]	<0.85	2.0	0.50
30	15.8	11.5	0.73	3.7	0.45	17.3	13.7	0.79	5.13	0.40
20	16.1	13.8	0.85	4.0	0.47	18.8	16.5	0.88	5.25	0.32
10	17.2	13.2	0.77	4.3	0.41	24.5	21.3	0.87	5.70	0.15
5	20.2	17.1	0.84	5.4	0.32	32.0	28.5	0.85	6.5	0.079
4	22.5	18.4	0.81	6.1	0.26	33.7	28.5	0.84	6.9	0.071
3	23.3	19.1	0.79	7.0	0.27	41.0	34.5	0.84	7.3	0.042
2.5	22.0	17.6	0.80	6.7	0.31	33.2	25	0.76	8.0	0.82
2	23.5	19.6	0.83	8.3	0.31	42.5	39	0.92	4.0	0.21
1	26.5	20.5	0.77	11.3	0.30	43.7	36	0.82	3.5	0.41
0.5	25.7	20.4	0.79	10.5	0.31	26.5	31.0	1.19	0.25	0.005
0	23.0	17.5	0.76	7.7	0.31	8.6	13.4	1.58	0.07	0.05

[a] R_g values smaller than 10 nm cannot be determined by light scattering with a reasonable accuracy, i.e., ±10%, because the angular dependence of the scattering intensity becomes less than 2% within the accessible *q* range.

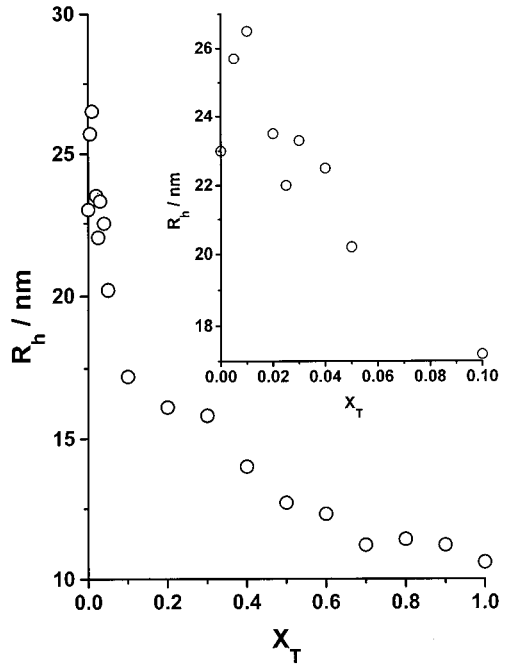

Figure 1. Hydrodynamic radius R_h for different content of cross-linking agent (T-units) in mole fractions of T-units, X_T, in aqueous dispersion.

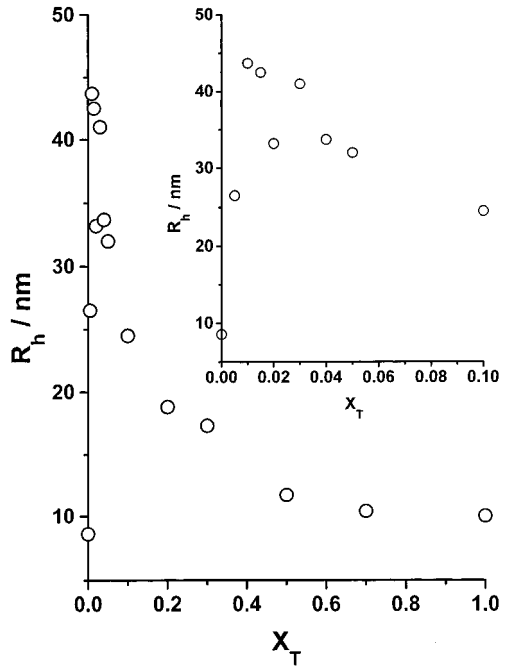

Figure 2. Hydrodynamic radii R_h for particles derived from the samples shown in Figure 1, swollen in toluene.

measurements of the endcapped particles in toluene (see Figure 2). This maximum might coincide with the intraparticle gelation threshold as indicated by the increased value of ρ_{LS} for the endcapped species in toluene as shown in Figure 3. This discontinuity was first believed to represent an experimental artifact but was absolutely reproducible in repeated experiments. At present no explanation for this peculiar behavior can be given.

Unfortunately the molar mass, M_w^D, of the aqueous dispersion particles is not easily accessible because the mass concentration of the dispersed particles decreases

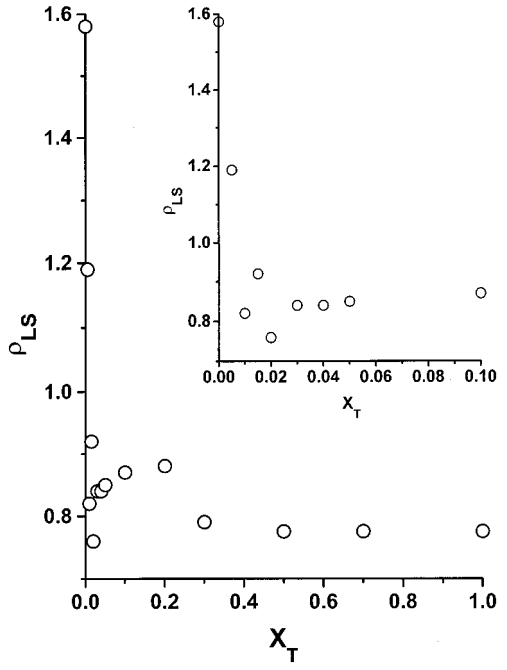

Figure 3. Ratio $\rho_{LS} = R_g/R_h$ for the μ-networks swollen in toluene.

with increasing conversion according to

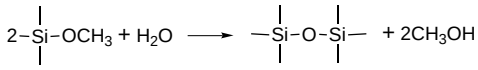

The molar mass of the dispersed micronetworks, M_w^D, and the conversion U given in Table 2 are derived from the increase in molar mass by the "endcapping" reaction, i.e.

$$H_2O + -Si-OCH_3 + X-Si(CH_3)_3 \rightarrow -Si-O-Si(CH_3)_3 + HX + CH_3OH$$

The conversion U and the molar mass, M_w^D, are determined by an iterative procedure in which the conversion is varied until the increase in molar mass caused by the endcapping reaction is matched (see Appendix). For such a calculation the contribution of the surfactant to the molar mass has to be subtracted which requires the assumption that all the surfactant is located on the particles. Thus, the molar mass M_w^D given in Table 2 represents the pure organosilicon molar mass in the dispersion and M_w the particle molar mass after the endcapping reation.

The resulting particle density in dispersion

$$\rho_d^D = \frac{3M_w^D}{4\pi {R_h}^3 N_L} \quad (1)$$

is observed to be constant and on the order of 1/3 of the bulk density. This small particle density favors the speculation that an "inner" surface exists inside of the dispersed particles. Even after the endcapping reaction a significant "free volume" persists in the presumably unswollen particles at T-contents larger than 50 mol % as indicated by the density ρ_d of the endcapped particles in solution defined in analogy to eq 1. At T-contents less than 50 mol % the particles swell, which is discussed below.

Table 3. Determination of the Flory Interaction Parameter χ from the Swelling Ratio According to the Various Theoretical Models for the Organosilicon μ-Networks in Toluene

		χ^a			
M_c	Q^c	Flory–Wall	Hermans	James–Guth	GDS[b]
173	1.47	0.44	0.73	0.62	0.94
296	1.78	0.34	0.55	0.54	0.61
666	3.22	−0.09	0.07	0.29	0.53
1406	4.35	−0.01	0.11	0.33	0.539
2392	5.89	0.00	0.08	0.33	0.47

[a] Calculated according to eq 2 with M_{lin} = 35 000 g/mol, V_s = 106.11 cm^3 mol, and ν_{sp} = 1.03 cm^3/g. [b] Graessley–Duiser–Staverman model. [c] Swelling ratio derived from the measured hydrodynamic radii, $Q \equiv [(R_h^{Tol} - b)/R_h^{H_2O}]^3$, with b the contribution of the surfactant to the particle radius in aqueous dispersion. From the data in Table 2, b = 0.6 nm for the nonswollen μ-network with 100% T-units.

The Swelling Behavior. The swelling behavior of micronetworks represents an interesting topic because the swelling is not influenced by macroscopic heterogeneities and mechanical defects. The theoretical expressions for the swelling ratio Q of networks prepared in bulk may be summarized as[4,6]

$$AQ^{5/3} - BQ = -\frac{\nu_{sp}}{V_s}\frac{M_c}{\left(1 - \frac{2M_c}{M_{lin}}\right)}Q^2[\ln(1 - Q^{-1}) + Q^{-1} + \chi Q^{-2}] \quad (2)$$

which reduces for large swelling ratii Q to

$$AQ5/3 - BQ = \frac{\nu_{sp}}{V_s}\frac{M_c}{\left(1 - \frac{2M_c}{M_{lin}}\right)}(0.5 - \chi) \quad (3)$$

In the equations above, M_c represents the number average molar mass between two cross-links, χ the Flory interaction parameter, V_s the molar volume of the solvent and ν_{sp} the specific volume of the μ-network. M_{lin} is the hypothetical primary chain molar mass which would be obtained in the absence of cross-linker; i.e., the term $2M_c/M_{lin}$ accounts for dangling ends. For the present experiments $M_{lin} = M_n \approx$ 35 000 g/mol (see Table 2).

The prefactors A and B vary according to different models: $A = 1$, $B = 2/f$ (Flory and Wall[7]); $A = 1$, $B = 1$ (Hermans[8]); $A = (f - 2)/f$, $B = 0$ (James and Guth [9]); $A = (f - 2)/2$; $B = 2/f$ (Graessley[10] and Duiser–Staverman[11]). As seen in Table 3, none of the models yield χ-values which are independent of the cross-linking density, i.e., the content of T-units. Only for the Graessley–Duiser–Staverman model do the extracted χ-values for the μ-network with the lowest cross-linking density come close to χ = 0.45 reported for PDMS/toluene in the literature,[12] but they become too large with increasing number of T-units. This discrepancy could originate from the increasing influence of the T-units on the thermodynamic behavior of the network or from the possibility that the cross-linking reaction might not have entirely taken place in bulk. More insight into this topic will be gained by rheological measurements which will be performed in the near future with particular emphasis on the influence of the micronetwork topology presented in the next paragraph.

Microstructure and Glass Transition. In Figure 5 the glass transition temperature T_g is plotted as function of the molar content of T-units, X_T. T_g is observed to increase linearly with increasing T-content as expected until above 50 mol % T-units no glass transition is observed anymore. Samples A–C shown in Figure 4 were simultaneously cocondensed; i.e., premixed D- and T-units were slowly and continuously dropped into the reaction flask. Although the cocondensation kinetics result from complex hydrolysis and condensation reactions, all of which depend on subtle electronic and steric effects[13] it seems safe to conclude that the cocondensed structures exhibit a more or less random branching topology.

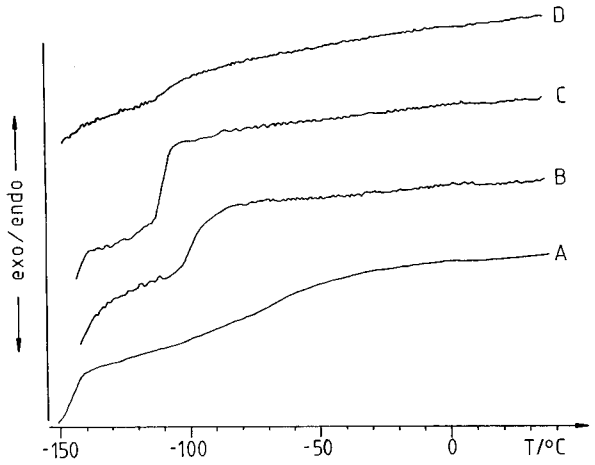

Figure 4. DSC-trace for particles of different network topology: (A) homogeneously cross-linked, X_T = 0.5; (B) homogeneously cross-linked, X_T = 0.2; (C) homogeneously cross-linked, X_T = 0.1; (D) core–shell particles with a core of linear chains (D-units) and a shell of pure T-units with the overall mole fraction X_T = 0.57.

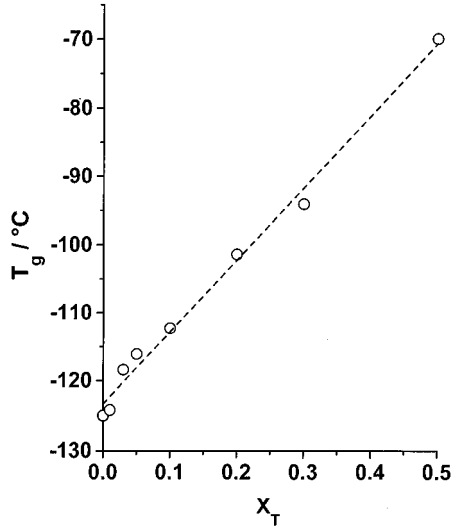

Figure 5. Glass transition temperature T_g for different mole fractions of T-units, X_T.

Core–Shell Structures. In order to produce an extremely heterogeneous micronetwork a precursor dispersion of pure D-units was prepared in a first step and reacted to complete conversion yielding linear PDMS chains. Subsequently, a layer of pure T-units is condensed onto the precursor dispersion. Table 4 comprises the particle characterization in aqueous dispersion and in organic solvents after the "endcapping" reaction.

The overall composition of the resulting micronetwork expressed in terms of the mole fraction of D-units, X_D, is calculated to X_D = 0.4305 under the assumption of

Table 4. Particle Characterization of the Core−Shell Topologies in Various Solvents

sample	solvent	R_h (nm)	R_g (nm)	ρ_{LS}	$M_w \times 10^6$ g/mol
	(a) Linear Core and Cross-Linked Shell				
core	10^{-4} *m* KBr	17.0	13.1	0.77	3.0
core−shell	10^{-4} *m* KBr	20.2	15.2	0.76	7.2[a]
core−shell	toluene	23.0	17.0	0.74	9.0[b]
core−shell	THF	20.0	19.5	0.98	5.0[c]
	(b) Cross-Linked Core and Linear Shell				
core	10^{-4} *m* KBr	8.3	<10	<1.2	0.5
core−shell	10^{-4} *m* KBr	11.0	<10	<0.9	0.86
core−shell	toluene	13.2	15.4	1.16	1.2

[a] Particle molar mass, no endcapping. [b] Particle molar mass, endcapped. [c] Molar mass of the shell, only.

full conversation of all functional groups (monomer weight ratio D/(D + T) = 0.4). This number compares well to the experimentally determined values: The comparison of the hydrodynamic radii measured from the aqueous dispersion before and after addition of the T-units yields the mass fraction of D-units $m_D = 0.41$ assuming that $m_D = R_h^3$(D-unit)/R_h^3(D- + T-units) which in turn leads to a mole fraction $X_D = 0.39$. Comparison of the molar masses measured in toluene (yielding the total particle mass) and in THF (which yields to the molar mass of the pure T-fraction, because THF is isorefractive with linear PDMS) leads to $m_D = 0.45$ resulting in a mole fraction $X_D = 0.42$.

The light scattering results also indicate a core−shell topology of the micronetworks as revealed by the ratio ρ_{LS}. In toluene both, the linear core and the cross-linked shell, significantly contribute to the radius of gyration and the ρ value for a sphere is obtained. In THF the linear core is invisible and R_g of a "hollow" sphere is measured. The resulting ratio $\rho_{LS} = 0.98$ is now close to the value of 1 theoretically expected for a hollow sphere. These results, however, do not strictly prove the postulated core−shell topology, because (i) a small polydispersity could increase ρ_{LS} as well and (ii) the structure seems to swell a little bit in toluene which is a better solvent for organosilicones than THF.

Final evidence for a core−shell topology is given by the DSC-trace. According to Figure 5 a microgel with composition $X_D = 0.43$ should exhibit a hypothetical T_g of −65 °C which should be most likely not observable because of the increasingly weak glass transition. Figure 4 shows the DSC trace of the core−shell particle (curve D) to exhibit a weak but noticable glass transition at $T_g = -107$ °C. According to the linear relation shown in Figure 5 this glass transition temperature extrapolates to $X_D = 0.85$ for a "homogeneously" cross-linked particle. Clearly, such a large X_D value is beyond the experimental uncertainty. The observed thermal behavior in combination with the light-scattering results discussed above is only compatible with a core−shell topology of the particles consisting of a core of linear chains embedded in a cross-linked shell of T-units.

At the moment we have no evidence to what extend the cross-linked shell is chemically bound to the linear chains in the core. However, the presented structure certainly constitutes a first step toward a supramolecular model system comprising a spherical micronetwork inside of which a certain number of linear chains are immobilized or "caught" by topological constraints, solely. Furthermore, such particles should exhibit interesting rheological properties because they should be viewed as "molecular soccer balls" the inner pressure of which could be created by the osmotic pressure of the linear chains, particularly if swollen in a nonvolatile solvent such as silicon oils.

Such core−shell structures could be incorporated into macroscopic networks via surface functionalization of the microgels and lead to well-defined networks of an extremely large, but well-defined, heterogeneity as well as to networks with rheologically active fillers. Such investigations are currently in progress.

Acknowledgment. Financial support from Wacker-Chemie GmbH, from the "Bayerischer Forschungsverbund Katalyse", and from the "Fond der Chemischen Industrie" is gratefully acknowledged.

Appendix

The determination of the molar mass and of the refractive index increment, d*n*/d*c*, is not easily performed, because the concentration of the dispersion is not exactly known. Moreover, the presence of surfactant introduces further complications which require some simplifying assumptions.

For the determination of the molar mass, we assume that the surfactant is exclusively bound to the particles; i.e., the amount of free surfactant is negligible. Then the particle molar mass is easily derived from the known fleet ratio *S*.

More laborious (and more speculative) is the determination of the precise particle concentration, because the concentration of the monomer (i.e., methyltrimethoxysilane) is known, but not the conversion of methoxy groups into Si−O−Si bonds. Assuming full conversion the weight loss amounts to 69 g/mol per reacted functionality because methanol is formed by the condensation reaction. The apparent quantities for d*n*/d*c* given in Table 1 are derived from concentrations calculated from the weighted monomer under the assumption of 100% conversion.

Since the true conversion is smaller, the actual mass concentration of particles is larger, i.e., $dn/dc < (dn/dc)^{app}$. The apparent molar mass is derived from the normalized scattering intensity R_θ by

$$M_w^{app} \sim \frac{R_\theta}{(dn/dc)_{app}^2 c_{app}} \tag{A1}$$

which leads to

$$M_w^{real} = M_w^{app} \frac{c_{real}}{c_{app}} \tag{A2}$$

The conversion *U* is now determined by an iterative procedure from the increase of the molar mass originating from the "endcapping" reaction which converts one methoxy group into $Si(CH_3)_3$, i.e. increases the molar mass per unreacted functionality. Starting from $U_1 = 0.5$ a molar mass $M_w(U_1)$ via $c(U_1)$ and the endcapped molar mass $M_w^{EC}(U_1)$ are calculated and the latter is compared to measured M_w of the endcapped particles in toluene solution. The procedure is repeated with increasing conversion U_i until the measured M_w and the calculated M_w^{EC} concide. The corresponding "true" particle molar mass in aqueous dispersion is listed in the respective tables above. However, the described procedure yields correct molar masses, only if all monomers are linked to a micronetwork particle; i.e., no sol fraction is lost by the precipitation and washing procedures. Thus, the reported molar masses

in aqueous solution (Table 2 and 4) should not be taken too seriously.

References and Notes

(1) Baumann, F.; Schmidt, M.; Deubzer, B.; Geck, M.; Dauth, J. *Macromolecules* **1994**, *27*, 6102.
(2) Baumann, F.; Deubzer, B.; Geck, M.; Dauth, J. *Adv. Mater.* **1997**, *9*, 955.
(3) Becker, A.; Köhler, W.; Müller, B. *Ber. Bunsen-Ges, Phys. Chem.* **1995**, *99*, 600.
(4) Antonietti, M.; Bremser, W.; Schmidt, M. *Macromolecules* **1990**, *23*, 3796.
(5) Wu, C. *Macromolecules* **1994**, *27*, 298.
(6) Mark, J. E. *Adv. Polym. Sci.* **1982**, *44*, 1.
(7) Flory, P. J.; Wall, F. F. *J. Chem. Phys.* **1951**, *19*, 1435.
(8) Hermans, J. J. *Trans. Faraday Soc.* **1947**, *43*, 591.
(9) James, H. M.; Guth, E. *J. Chem. Phys.* **1943**, *11*, 455; **1953**, *21*, 1039.
(10) Graessley, W. W. *Macromolecules* **1975**, *8*, 189; **1976**, *9*, 865.
(11) Duiser, J. A.; Staverman, J. A. *Physics of non-crystalline Solids*; North Holland: Amsterdam, 1965.
(12) Chahel, R. S; Kao, W.-P.; Patterson, D. *J. Chem. Soc., Faraday Trans.* **1973**, *69*, 1834.
(13) Sanchez, V.; McCormick, H. *Chem. Mater.* **1190**, *3*, 320.

MA970415D